Molecular Immunology 111 (2019) 128–135

Contents lists available at ScienceDirect

Molecular Immunology

journal homepage: www.elsevier.com/locate/molimm

A critical challenge in the development of antibody: Selecting the appropriate fragment of the target protein as an antigen based on various epitopes or similar structure

Mahboubeh Razzaqi[a], Mohammad Javad Rasaee[a,*], Maliheh Paknejad[b]

[a] Department of Medical Biotechnology, Faculty of Medical Sciences, Tarbiat Modares University, Tehran, Iran
[b] Department of Biochemistry, Faculty of Medicine, Tehran University of Medical Sciences, Tehran, Iran

ARTICLE INFO

Keywords:
PKM2
In silico analysis
3D structure
Truncated antigen
Antibody development
Monoclonal antibody

ABSTRACT

The main challenge in the development of antibody is to select the appropriate antigen particularly when a truncated protein is used for immunization or as vaccine antigen. In previous studies, fragment selection was mainly based on epitopes and less often on the structure. Fewer studies have paid attention to the prediction of the truncated protein 3D structure and retained its similarity in the native and truncated proteins. Here we used in silico analysis to select two fragments of Pyruvate Kinase M2 (PKM2), as a tumor marker. One fragment, M-tPKM2, had a shorter sequence with one epitope although the predicted 3D structure was similar to the native PKM2. The other fragment, R-tPKM2, had a longer sequence and thus more epitopes, but had a different structure from the native PKM2. Recombinant truncated proteins were expressed in E. coli and purified via affinity chromatography. Secondary structure elements in purified proteins were determined by Circular Dichroism, then they were utilized to develop antibodies in mice. Both antigens could elicit high immune response against themselves (OD_{450} = 3.326 ± 0.562 for M-tPKM2; OD_{450} = 3.562 ± 0.110 for R-tPKM2). However, significantly higher response against PKM2 was observed among the mice immunized with M-tPKM2 ($p < 0.0001$ by One way ANOVA followed by Tukey's post hoc comparison). Also, the monoclonal antibody produced against the M-tPKM2 could recognize the native PKM2 in the MCF7 cells. Our finding suggested that for the purpose of designing an antigen with the ability to produce a potent antibody against the target protein, it is better to select sequences which have a similar structure in truncated and native proteins, even at the cost of having shorter sequences and fewer epitopes.

1. Introduction

Selecting the appropriate fragment of the target protein as an antigen is a critical challenge that faces researchers in the first step of antibody development or vaccine design since the antibody produced against the truncated protein must be able to detect the native protein. Having utilized in silico studies, it is possible to predict the desired protein features which may reduce the amount of experimental analyses (Leach, 2001). Several factors are involved in this approach. In most studies, fragment selection is based on the evaluation of the target protein sequence. The sequence was used to identify the potentially immunogenic epitopes (Xi and Whittaker, 2017; Aa, 2017) and similar sequences between target proteins and others (Bielecka et al., 2015). Fewer studies have paid attention to the three-dimensional (3D) structure of the selected fragment in the native protein, but most of them disregarded the prediction of the truncated protein 3D structure and retained its similarity in the native and truncated proteins. In some studies, the identification of the truncated protein via the antibody generated against the native protein is considered as a sign of the structural similarity between truncated and native proteins (Amorim et al., 2012). Sometimes, truncated protein ability to bind the receptor is regarded as the similarity of the structure (Fischer et al., 2016). Prediction of different truncated protein structures and comparison of their properties to select from among them have been used by other researchers as a strategy (Bameri et al., 2018). In a few studies, the probable conformation of the truncated protein has been predicted and its similarity with native protein structure has been used for fragment selection (Fonseca et al., 2016; Shabani et al., 2017).

In this study, to further evaluate the effects of various factors involved in the antigen design on the antibody ability to detect the native

* Corresponding author at: Department of Medical Biotechnology, Faculty of Medical Sciences, Tarbiat Modares University, Jalal Ale Ahmad Highway, PO Box 14115-331, Tehran, Iran.
E-mail address: rasaee_m@modares.ac.ir (M.J. Rasaee).

https://doi.org/10.1016/j.molimm.2019.04.018
Received 5 October 2018; Received in revised form 3 January 2019; Accepted 23 April 2019
Available online 01 May 2019
0161-5890/

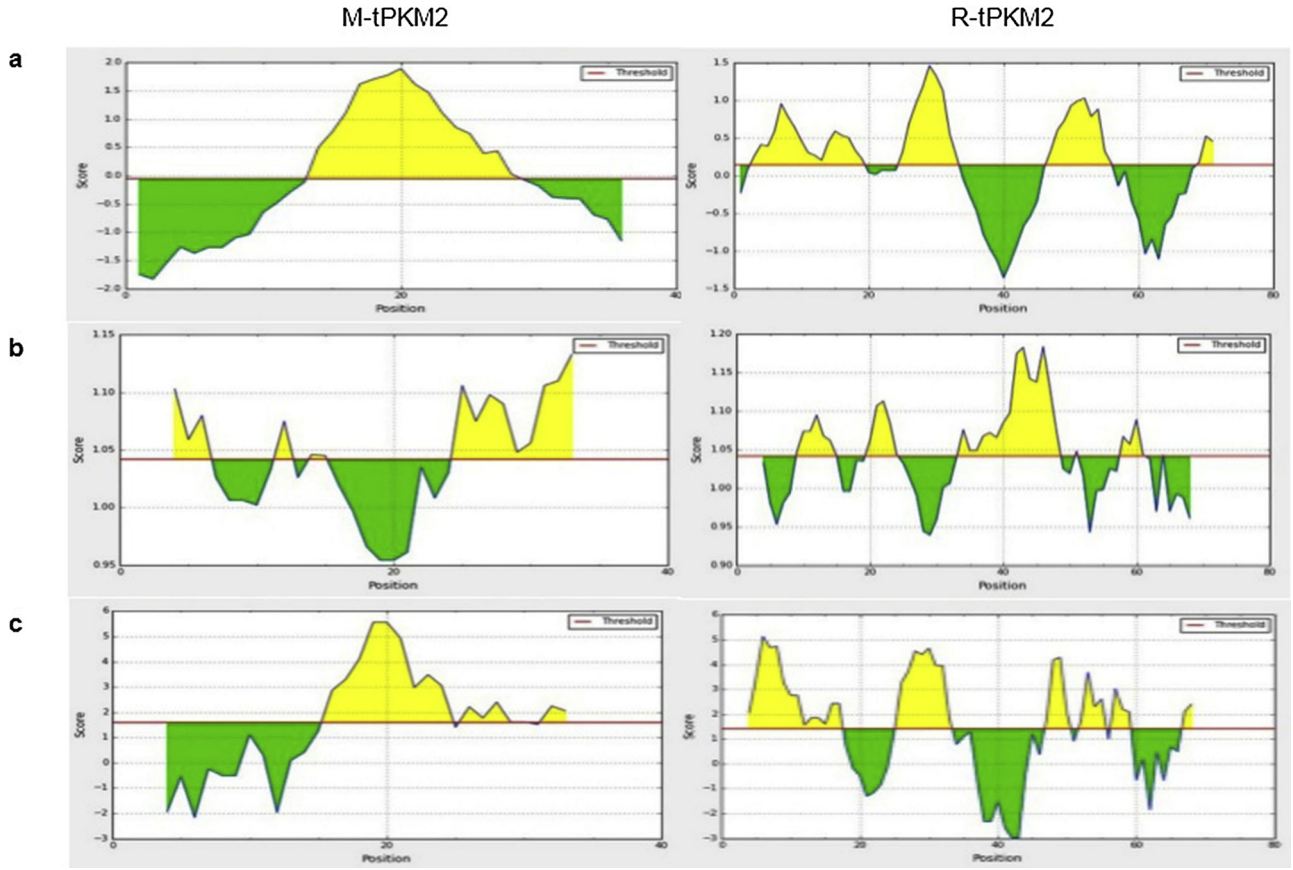

Fig. 1. B cell epitope prediction (a), antigenicity (b) and hydrophilicity (c) of M-tPKM2 and R-tPKM2. Horizontal line is the threshold. Below the threshold denotes unfavorable regions related to the properties of interest. Above the threshold, indicate favorable regions consisted of higher scored residues.

protein, we chose Pyruvate Kinase M2 (PKM2) as target protein. The PKM2 isoform is encoded and overexpressed in tumor cells, and its presence is vital for their proliferation (Dayton et al., 2016). PKM2 is also a prognostic marker for different cancers and its overexpression associated with poor prognosis (Chen et al., 2015; Cui and Shi, 2015). We selected two fragments of the PKM2 based on the number of epitope and predicted 3D structure. The first fragment had a shorter sequence with one epitope and the predicted 3D structure was similar to the native PKM2. The second one had a longer sequence and various epitopes, although prediction of its 3D structure was not similar to the native PKM2. Selected fragments were expressed in E. coli and purified as recombinant truncated proteins which were used for immunization. In silico and in vitro properties of antigens and the produced antibodies' ability to detect the PKM2 were evaluated. The possibility of identifying the PKM2 in tumor cells was also examined by using the monoclonal antibody.

The results of this study can be used to improve our understanding of the antigen selection for antibody development via in silico analysis.

2. Materials and methods

Unless stated otherwise, all reagents were catered from Sigma (Sigma-Aldrich, St. Louis, MO, USA).

2.1. In silico design of truncated PKM2

The complete sequence of PKM2 (**accession no. p14618**) and the crystal structure data (**PDB ID: 1T5A**) was used for analysis. IEDB analysis resource (http://www.iedb.org) was applied for more investigation of the sequence: Bepipred linear epitope, antigenicity and hydrophilicity prediction were used for the identification of the potential B cell epitopes and selecting the appropriate sequences; T cell epitope prediction tools were utilized; Conformational B cell epitopes were predicted using DiscoTope 2.0. Based on these sequence analyses, two fragments, M-tPKM2 and R-tPKM2 were selected. Antigen probability of these fragments was estimated by VaxiJen (http://www.ddg-pharmfac.net/vaxijen/VaxiJen/VaxiJen.html). Predicted solubility upon overexpression was calculated by Scratch Protein Predictor (http://scratch.proteomics.ics.uci.edu/).

2.2. Analysis of recombinant proteins

The final sequences of selected fragments in expression vectors were considered for further evaluation. For M-tPKM2 and R-tPKM2, pET-28a (+) and pET-32a(+) (Novagen, Madison, WI, USA) were utilized, respectively. The ExPASy ProtParam (https://web.expasy.org/protparam) was used to measure the physico-chemical parameters of the recombinant proteins. The sequences were back-translated to DNA and optimized for expression in Ecoli using gene optimization software (https://eu.idtdna.com/CodonOpt). Codon Adaptation Index (CAI) (https://www.biologicscorp.com/tools/CAICalculator/), and GC content (https://www.biologicscorp.com/tools/GCContent/) were calculated as an approximate indicator of the likely success of the heterologous gene expression.

2.3. Secondary and tertiary structure prediction

The PSIPRED server secondary structure prediction method (http://bioinf.cs.ucl.ac.uk/psipred/) was used to predict and analyze the secondary structure of recombinant truncated proteins. The 3D structure of these proteins were predicted by using the I-TASSER server (http://zhanglab.ccmb.med.umich.edu/I-TASSER/). The quality and reliability

Table 1
The physico-chemical characteristics of two recombinant truncated proteins.

Recombinant truncated protein	Number of aa[a]	MW[b](KDa)	pI[c]	negatively charged residues (Asp + Glu)	positively charged residues (Arg + Lys)	Extinction Coefficient (with/without Cys)[d]	Half-life in Ecoli	Instability Index[e]	Aliphatic Index	GRAVY[f]
M-tPKM2	135	14.26	6.55	14	11	3230/2980	> 10h	37.96	64.00	−0.296
R-tPKM2	241	26.26	6.99	29	28	22585/22460	> 10h	20.39	77.39	−0.458

[a] aa: Amino Acid.
[b] MW: Molecular Weight.
[c] pI: Isoelectric point.
[d] Extinction coefficients are in units of M^{-1} cm^{-1}, at 280 nm measured in water.
[e] A protein whose instability index is smaller than 40 is predicted as stable.
[f] Grand average of Hydropathicity.

Table 2
Comparison of secondary structure prediction of M-tPKM2 and R-tPKM2 by PSIPRED server with secondary structure content obtained from CD data.

	M-tPKM2 (%)		R-tPKM2 (%)	
	Predicted	CD data	Predicted	CD data
Helix	53.3	68	29	31.1
Sheet	3	4.8	15.4	16.2
Random coil	43.7	27.2	55.6	52.7

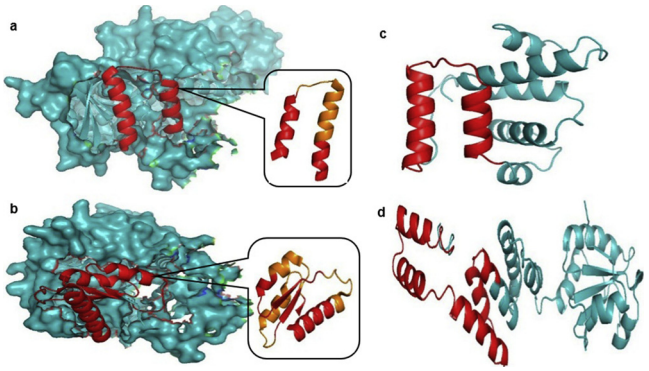

Fig. 2. Tertiary structure of M-tPKM2 (a) and R-tPKM2 (b) fragments in native PKM2 and predicted 3D structure of recombinant truncated M-tPKM2 (c) and R-tPKM2 (d). M -tPKM2 and R-tPKM2 fragments are shown darker (red) in ribbon style (B cell epitopes of these fragments are colored in orange). The lighter regions (blue) are represented other parts of native PKM2 and recombinant truncated proteins. As shown, unlike the R-tPKM2, the 3D structure of the M-tPKM2 sequence in native PKM2 is preserved in the recombinant truncated model (For interpretation of the references to colour in this figure legend, the reader is referred to the web version of this article).

of modeled structures were validated and evaluated using RAMPAGE (http://mordred.bioc.cam.ac.uk/~rapper/rampage.php) and ProSa (https://prosa.services.came.sbg.ac.at/prosa.php) server. Visualization of 3D structures were carried out by PyMOL software, version 2.0.

2.4. Preparation of recombinant truncated proteins

The M-tPKM2 and R-tPKM2 genes were synthesized with the hexa-histidine (His)-tag at their C-terminal site (Biomatik Company, Canada), and inserted into the expression vectors. The resulting plasmids, pET28a/M-tPKM2 and pET32a/R-tPKM2, were transformed into E. coli BL21 (DE3) competent cells (Novagen, Madison, WI, USA). E. coli harboring the recombinant expression plasmids was cultured and induced by adding IPTG. Then induced bacteria were collected and the cell pellets were re-suspended in ice-cold lysis buffer (20 mM NaH2PO4, 500 mM NaCl and 20 mM imidazole, pH 7.4). Lysozyme (0.5 $mg.ml^{-1}$) and PMSF 1 mM were added and incubated on ice for 30 min with gentle shaking. Afterwards, the cells were lysed on ice by sonication and centrifuged at 10,000 × g at 4 °C for 30 min.

The supernatants were incubated with an equilibrated Ni-NTA resins (Qiagen, Hilden, Germany) for 2 h at room temperature, then the resins were washed with a 5-column volume of washing buffers (20 mM NaH2PO4, 500 mM NaCl and 20 mM imidazole, pH 7.4). The washing step was repeated with the same buffer containing 50 and 90 mM imidazole. Finally, the bound proteins were eluted by adding elution buffer (20 mM NaH2PO4, 500 mM NaCl and 500 mM imidazole, pH 7.4). The concentration of the proteins were determined using Bradford assay (Bradford, 1976) with bovine serum albumin (BSA) as standard protein to set up a standard curve. Fractions containing the proteins were pooled and concentrated using an Amicon® Ultra centrifugal filters 3000 MWCO. The recombinant truncated proteins were then dialyzed against Phosphate Buffered Saline (PBS, pH 7.4) and stored at

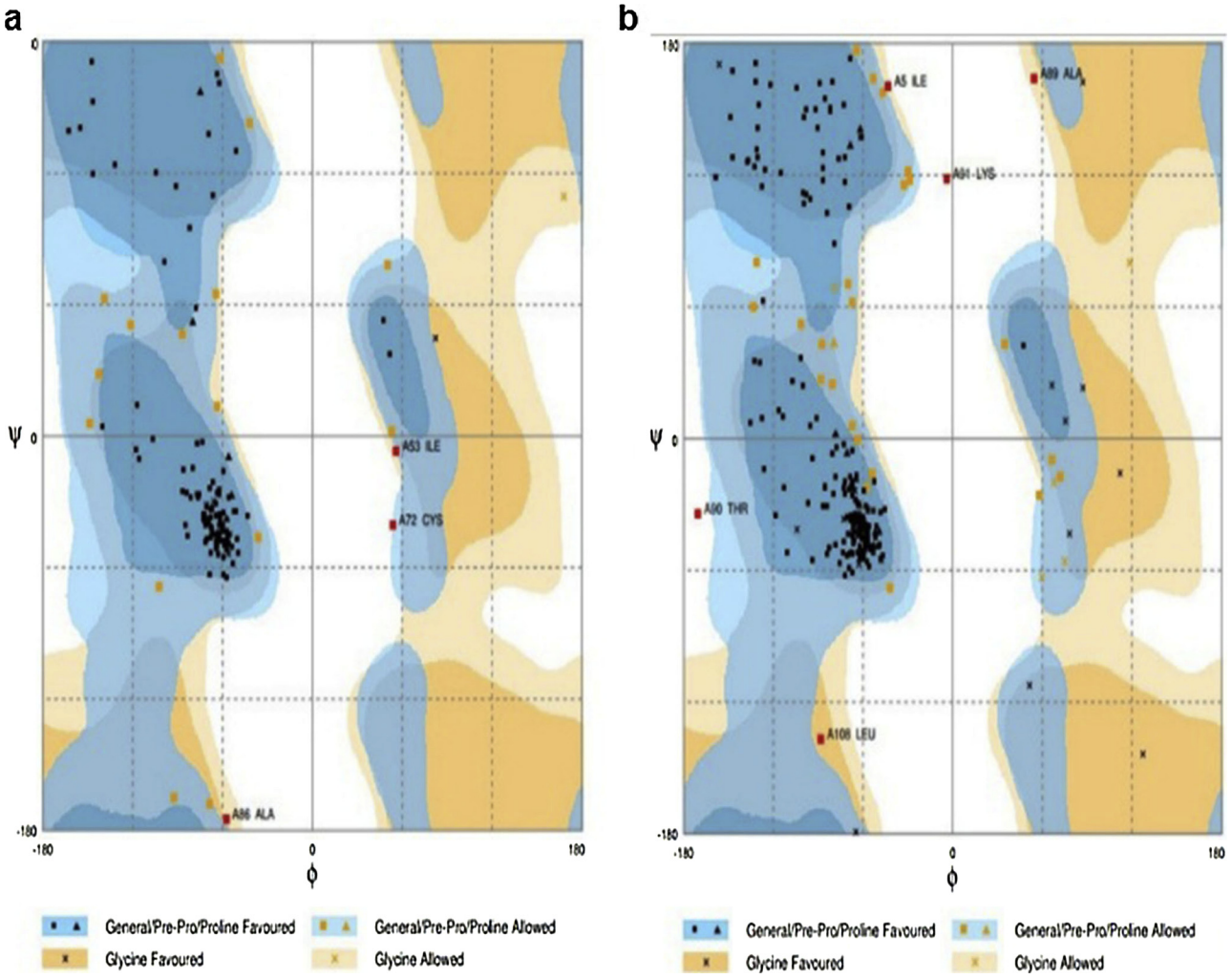

Fig. 3. Validation of recombinant truncated M-tPKM2 (a) and R-tPKM2 (b) by Ramachandran plot using RAMPAGE server. It determined that for M-tPKM2, 114 residues (85.7%) were located in the favored region, 16 residues (12%) in the allowed region, and 3 residues (2.3%) in the outlier region. Almost similar to R-tPKM2, 205 residues (85.5%) are estimated in the favored region, 29 residues (12.1%) in the allowed region, and 5 residues (2.1%) in the outlier region. Based on these results, 96.6% of the residues of both proteins were in acceptable regions.

−80 °C. Protein samples were analyzed by SDS PAGE under reducing conditions using standard protocols.

2.5. Circular dichroism (CD) measurement

The secondary structure elements present in the recombinant truncated proteins were measured by using a Jasco J-810 spectrometer (Jasco, Tokyo, Japan). The far-UV CD spectra (190–240 nm) were recorded at room temperature in a 1 mm path length cuvette at a protein concentration of 0.2 $mg.ml^{-1}$ in PBS, pH 7.4. The percentage of the secondary structures was calculated.

2.6. Immunization of mice by recombinant truncated proteins

Ethics approval for all experiments was granted by the animal ethics committee of the faculty of medical sciences, Tarbiat Modares University. The animals in the study were housed and used strictly in accordance with the guidelines of the EU Directive 2010/63/EU for animal experiments.

BALB/c female mice (6–8 weeks old) were purchased from the Pasteur Institute of Iran. The mice were immunized at the interscapular area by subcutaneous injections of 50 µg of recombinant truncated proteins emulsified in complete Freund's adjuvant for the primary injection and 25 µg of constructs incorporated in incomplete Freund's adjuvant for booster injections. The primary injection was followed by four boosts with fortnightly intervals and the mice were bled on day 0 (pre-immune) and one week after the third and fourth boosts. In the control groups, the mice were injected with PBS in the same adjuvant. ELISA was used to confirm that the produced antibodies in mice sera could react with their antigen (the M-tPKM2 or R-tPKM2) and absorbance was read at 450 nm (OD_{450}) using microplate reader (BioTek, Winooski, VT, USA). Also, the ability of these antibodies to detect PKM2 has been investigated.

The results were presented as mean OD ± standard deviation. Data were analyzed by One way ANOVA followed by Tukey's post hoc comparison, if there was an overall statistically significant difference in group means (p value ≤ 0.05).

2.7. Assessment of monoclonal antibody ability to recognize the native PKM2 in tumor cells

The mouse with the highest reactivity to the PKM2 was given an IV injection of 20 µg of the M-tPKM2 in PBS, four days before fusion. The mouse's splenocytes were fused with the Sp2/0 myeloma cells using standard methodology. Resulting hybridomas supernatants were screened for reactivity toward native PKM2 with ELISA. The stable hybridomas secreting antibodies specific to native PKM2 were subjected to limiting dilution culture, and the most productive and stable

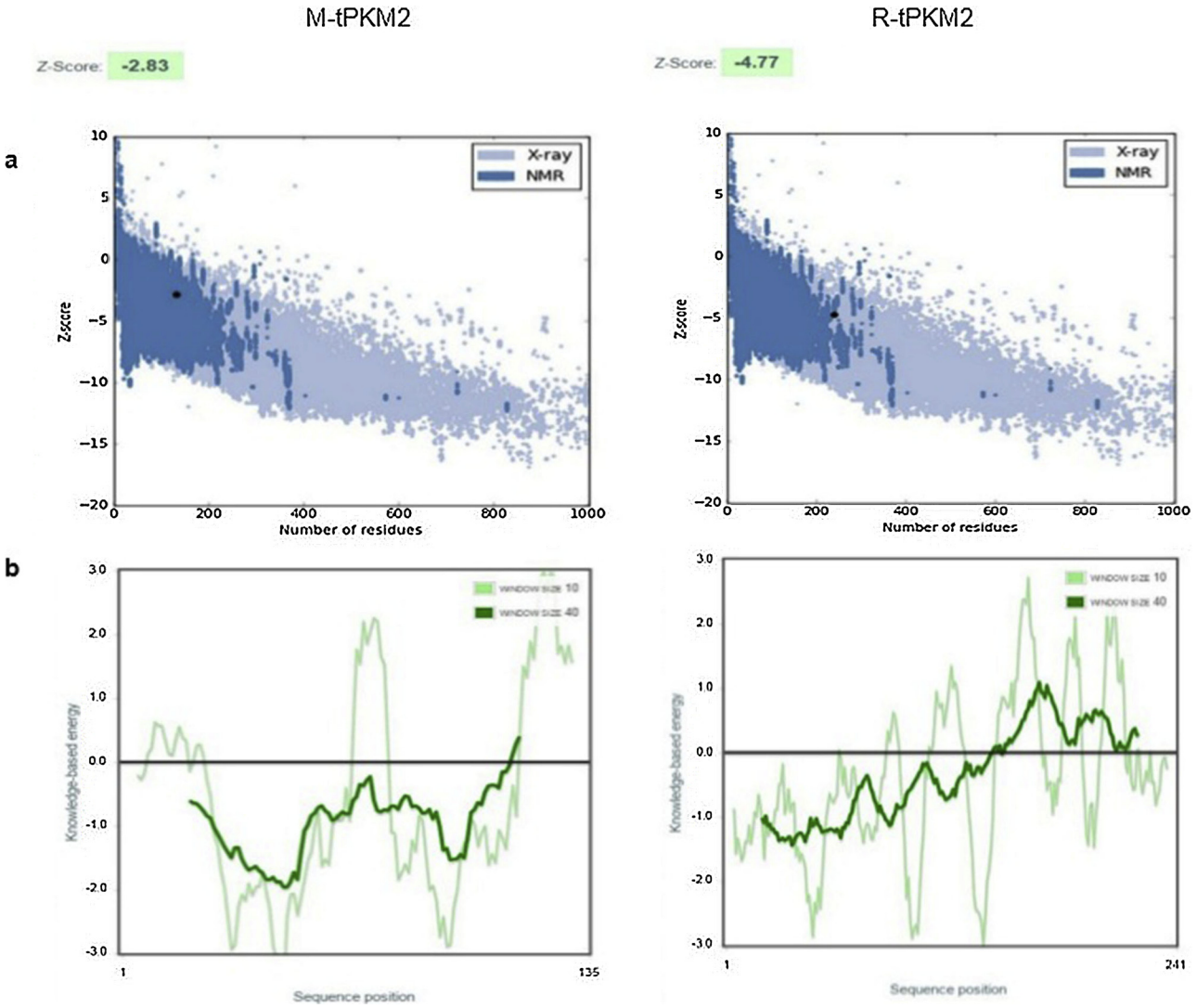

Fig. 4. Validation of recombinant truncated proteins via ProSa server. (a) The Z score (black dot) of both proteins were within the range of scores, typically found for the native proteins of a similar size. (b) The energy plot (dark line) shows the local model quality and positive values correspond to problematic or erroneous parts of the input structure. As indicated for M-tPKM2, overall the residue energies were largely negative.

clone was selected for monoclonal antibody production. IsoStrip mouse monoclonal antibody isotyping kit (Roche, Germany) was used to determine the class and subclass of monoclonal antibody.

Afterward, MCF7 cells were cultured to approximately 80% confluence, then washed with ice-cold PBS and removed by treatment with Trypsin-EDTA. The collected cells were lysed and total protein was extracted via incubation with RIPA buffer containing 1 mM PMSF (1 ml buffer for 10^7 cells) for 30 min on ice. Subsequently, the cells were centrifuged, the supernatant's total protein concentrations were determined using the Bradford assay (Bradford, 1976) and were stored at −20 °C. The ability of the monoclonal antibody to recognize the PKM2 in the MCF7 lysate was determined via western blot assay.

3. Results

3.1. In silico analysis of the truncated sequences

The PKM2 sequence analysis showed that only 9 out of 531 amino acids were conformational B cell epitopes. Thus, in order to exclude the conformational epitopes factor tampering with the evaluation of the fragments' 3D structure effect on the properties of the produced antibodies, the fragments were selected from regions that did not include conformational epitopes. Based on the in silico analysis of the PKM2 sequence and structure, we selected two fragments of PKM2 sequence as truncated proteins. The first fragment, M-tPKM2, consisted of 36 amino acids and the second one, R-tPKM2, had 71 amino acids. The results of antigenicity, hydrophilicity and B cell epitope prediction of selected fragments are shown in Fig. 1. The average score of hydrophilicity for the M-tPKM2 was 1.595, and this fragment had one B cell epitope with 14 amino acids length. For R-tPKM2, the average score of hydrophilicity was 1.422 and it had three epitopes with overall length of 36 residues. Therefore, the R-tPKM2 contained more amino acids that can act as an epitope. Also, the predictions of the peptide binding to MHC class II molecules, which is necessary to be recognized by the T cells, revealed that M-tPKM2 had slightly higher affinity. Furthermore, the antigen probability of the M-tPKM2 was predicted as 0.7441 and the assigned score for R-tPKM2 was 0.7260. The predicted solubility upon overexpression indicated that M-tPKM2 and R-tPKM2 were soluble with the probability of 0.87006 and 0.91045, respectively.

3.2. Analysis of recombinant truncated proteins properties

The complete results of physico-chemical parameters of M-tPKM2 and R-tPKM2 was shown in Table 1. In accordance with the instability

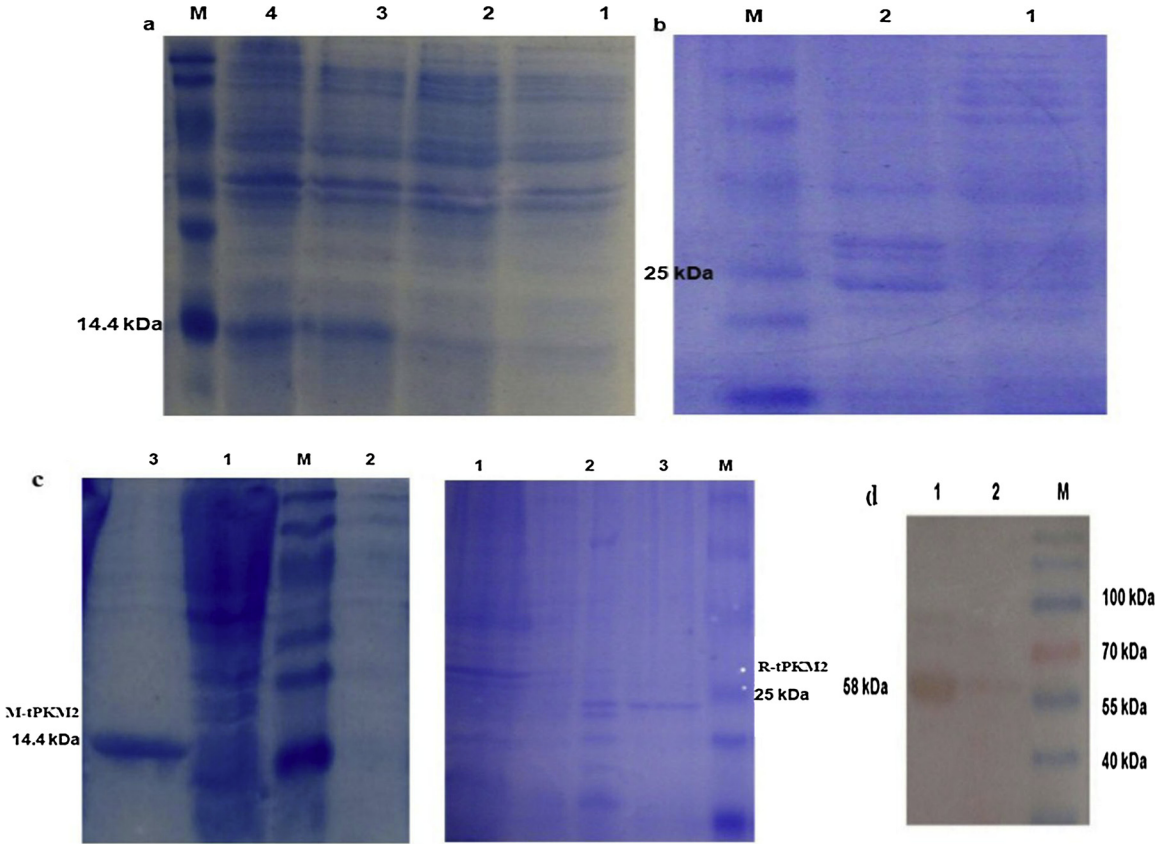

Fig. 5. SDS PAGE analysis of recombinant truncated proteins, (a) M-tPKM2 and (b) R-tPKM2: Lane M, molecular weight marker; lane 1, before transformation; lane 2, before induction; lane 3 and 4, after induction. (c) M-tPKM2 and R-tPKM2 were purified using Ni-NTA affinity column and analyzed by SDS-PAGE. For both proteins: Lane M, molecular weight marker; lane 1, flow-through; lane 2, washing; lane 3, elution (purified protein). (d) Western blot analysis of monoclonal antibody against M-tPKM2 with MCF7 lysate. Lane M, molecular weight marker; lane 1, PKM2; lane 2, MCF7 lysate. As indicated, the antibody could identified the PKM2 (58 KDa) in tumor cells lysate.

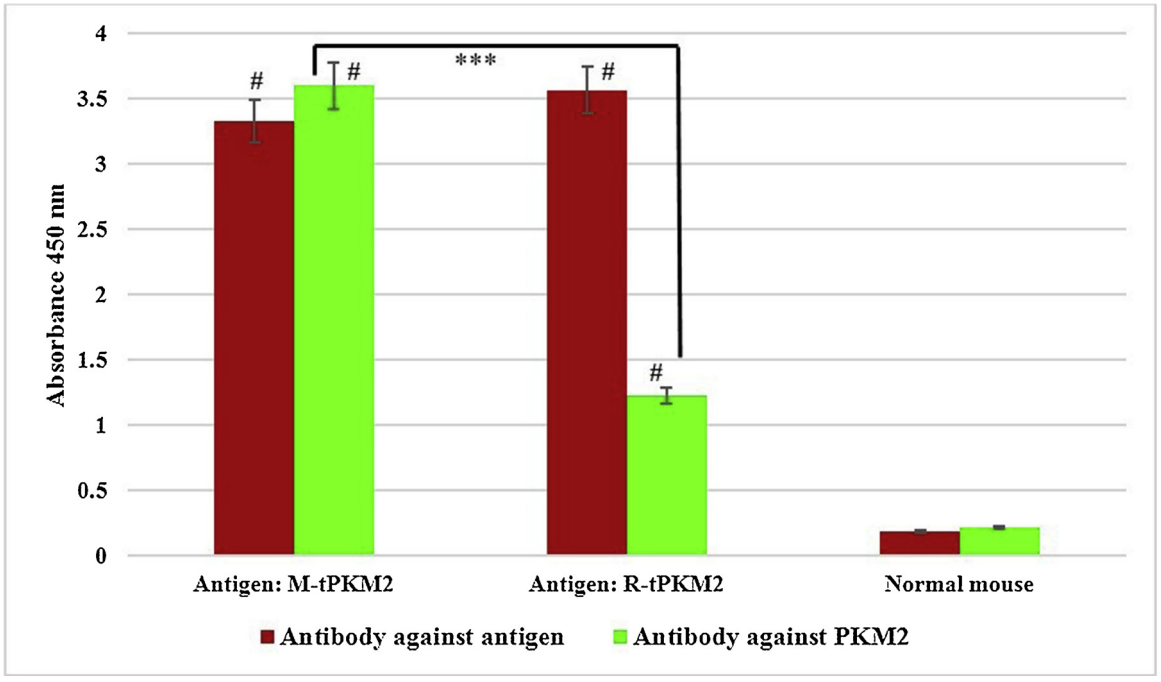

Fig. 6. Assessment of immune responses in mice immunized with M-tPKM2 and R-tPKM2 by ELISA. The reactivity of sera samples with recombinant truncated proteins (antigens) and PKM2 was comparable with the results earned from the control mice (#p value < 0.0001). Although the antibody responses are nearly similar to their antigens (M-tPKM2 and R-tPKM2), but differ with the native PKM2 (***p value < 0.0001).

index, both M-tPKM2 and R-tPKM2 were categorized as stable proteins and in vivo half-life of both proteins were estimated as > 10 h in E. coli.

The possibility of the high protein expression level is correlated with the value of CAI, and a CAI between 0.8–1 is considered as a good expression (Gustafsson et al., 2012). Furthermore, the GC content is considered as a measure value for the transcriptional and translational efficiency, where a range between 30–70% is a desired value (Newman et al., 2016). In this study, after optimization, these values were 0.78 and 58% for the M-tPKM2, which were higher than the R-tPKM2 values (0.60 and 50%).

The results of secondary structure prediction are shown in Table 2. Briefly, M-tPKM2 had 53.3% alpha helix and 3% beta strands, and R-tPKM2 possessed 29% alpha helix and 15.4% beta strands. The predicted secondary structure of the M-tPKM2 was almost similar to its native secondary structures. However, for R-tPKM2, it had less helix and beta strands than native. The tertiary structure of the selected fragments in full length PKM2 are schematically represented in Fig. 2a,b. The best tertiary models predicted for two recombinant truncated proteins (Fig. 2c,d) revealed that unlike the predicted structure of the R-tPKM2, the 3D structure of the M-tPKM2 sequence in native PKM2 is preserved in the recombinant truncated model.

Among predicted 3D structure models suggested from I-TASSER, the proper model was selected based on the C-score (confidence score) for estimating the quality of the predicted model which is typically in the range of -5 to 2 (a higher score is better) (Yang et al., 2014) and the M-tPKM2 had a better quality structure (M-tPKM2: 0.25; R-tPKM2: -0.12).

The Ramachandran plot was calculated by RAMPAGE server and based on these results, 96.6% of the residues for both proteins were in acceptable regions (Fig. 3). Additionally, the Z-score of both proteins (−2.83 for M-tPKM2 and −4.77 for R-tPKM2) were within the range of scores typically found for the native proteins of a similar size (Fig. 4a), which indicated that the predicted structures would be reliable models with a high quality. As Wiederstein and Sippl described, “the energy plot shows the local model quality by plotting energies as a function of amino acid sequence and positive values correspond to problematic or erroneous parts of the input structure” (Wiederstein and Sippl, 2007). As shown in Fig. 4b, unlike the M-tPKM2, for the R-tPKM2, large parts of the energy plot showed highly positive energy values which were located at the C-terminal of the sequence (including R-tPKM2 fragment).

3.3. Expression and purification of recombinant truncated proteins

The optimum expression of the soluble truncated proteins was obtained by adding 0.1 mM IPTG and incubation for 18 h at 18 °C. The SDS PAGE analysis showed specific bands at the size of approximately 14 and 26 kDa for M-tPKM2 and R-tPKM2, respectively (Fig. 5a,b). In addition, a higher expression of a soluble fraction was observed for recombinant truncated M-tPKM2 in comparison with the recombinant truncated R-tPKM2.

In order to maintain the recombinant proteins folded states, the soluble fraction of expressed proteins were purified using Ni-NTA resins (Fig. 5c). Due to the concentration of the purified proteins, the yield of the purified proteins for M-tPKM2 and R-tPKM2 were about 30 $mg.L^{-1}$ and 5 $mg.L^{-1}$ of the culture media, respectively.

3.4. Structural characterization of the recombinant truncated proteins

CD was performed to investigate the secondary structure properties of the purified proteins (Table 2). The CD data analysis of the M-tPKM2 revealed that it had a high content of helical structure, which is similar to those obtained by the PSIPRED server. However, the amount of helix and coil relative to the predicted value was higher and lower, respectively. As for the R-tPKM2, the CD data showed that similar to the prediction of the secondary structure, a high percentage of the protein contained random coil, representing less folding of the protein.

3.5. Development and assessment of polyclonal and monoclonal antibody

After fourth boosts, antibody response in the sera against M-tPKM2, R-tPKM2 and PKM2 were determined by ELISA. The mean OD ± standard deviation against their antigens in mice immunized with M-tPKM2 and R-tPKM2 were 3.326 ± 0.562 and 3.562 ± 0.110, respectively. As indicated in Fig. 6, there was a statistically significant difference between immunized mice (#) and control group as determined by one-way ANOVA ($p < 0.0001$) followed by Tukey’s post hoc test. Although the difference between the mean OD against truncated antigens was not significant ($p = 0.646$), the reactivity of these antibodies to the PKM2 was very different (***) and the ability of antisera raised against M-tPKM2 to detect the native PKM2 were significantly higher than those induced by R-tPKM2 (3.6 ± 0.1 for M-tPKM2; 1.227 ± 0.113 for R-tPKM2, $p < 0.0001$).

Also, to confirm the antibody's ability to detect the native PKM2 in tumor cells, the most immunized mouse (against M-tPKM2) was used to produce monoclonal antibodies which was determined to have an IgM/kappa isotype. The reactivity of the monoclonal antibody to the MCF7 protein extract was determined in a western blot assay which gave a specific reaction to the PKM2 at approximately 58 kDa (Fig. 5d). These findings showed that the antibodies against the M-tPKM2 are able to recognize the native PKM2 present in the tumor cells.

4. Discussion

The appropriate selection of fragment from target protein as antigen can be based on various factors such as B cell epitopes, sequence similarity, function of the desired fragment and 3D structure of fragment. In this work, we selected two fragments of the PKM2 sequence based on the number of epitopes and predicted 3D structure via in silico design, and evaluated the impact of these truncated antigens’ properties on the ability to detect native PKM2 by produced antibodies.

Identification of B cell epitopes is crucial for antigen design and longer sequences could be better because they could include more epitopes. In concordance with this assumption, in most of the previous studies, the sequences with long length were chosen to be used as truncated proteins (Xi and Whittaker, 2017; Yang et al., 2015). However, it should be noted that longer sequences could pursue their own specific conformation which may not be similar to the conformation of the sequence within the native protein. In our study, the length of the R-tPKM2 sequence was selected nearly twice the length of another fragment (M-tPKM2) to evaluate the effect of the longer length and multiple epitopes on the produced antibodies. Contrary to the common assumptions, the antibodies produced against the shorter sequence (M-tPKM2) with only one epitope had a higher ability to identify the target protein (Fig. 6). Our findings could be due to the fact that M-tPKM2 had secondary structure similar to its native structure, and most of them were alpha helix (Table 2) which would be regarded as a desired property. It is because the helical regions often maintain their structures which were confirmed via CD analysis. Also the 3D structure similarity of the M-tPKM2 fragment between native and recombinant truncated protein (Fig. 2a,c) could significantly improve the antibodies’ ability to detect native protein (Fig. 6). In line with our observation, in the study designed to select between two recombinant truncated fragments of Plasmodium vivax MSP-1, the MSP-119 with 98 amino acids had better reactivity with all of the sera collected from P.vivax-infected patients compared to the MSP-142 with 430 residues (Sachdeva et al., 2004).

The sequence analysis of the truncated proteins indicated that for both proteins the average score of antigenicity and hydrophilicity were almost similar (Fig. 1), and these findings were confirmed in the ELISA result with the recombinant truncated proteins (Fig. 6).

Although the predicted solubility for both truncated proteins were soluble with high probability, the R-tPKM2 were appeared to be very insoluble and expressed as an inclusion body. This is despite the use of pET-32a(+) as an expression vector which had thioredoxin (TRX) tag

to increase the solubility and assist in the proper folding of protein. In agreement with these results, in a study by Mohanty NN, et al, the truncated NS3DHD gene was inserted into a pET32a vector and the expression resulted in insoluble proteins (Mohanty et al., 2016). As shown in the Fig. 4b, the highly positive energy values at the C-terminal of the sequence could be a reason for the insoluble expression of the R-tPKM2. Also, according to the secondary structure prediction more than half of the R-tPKM2 structure had an unordered conformation. Similar results were obtained in CD evaluation (Table 2). These findings could lead to the assumption that the R-tPKM2 with a different structure from that of the native tends to be less ordered which might affect the soluble expression of the protein. In addition, it seems that the higher expression level in the case of M-tPKM2 could be explained by a better CAI and GC content. In accordance with our results, in the study of Knight and his colleagues, it was shown that changing factors like codon usage optimization and GC content will lead to improved mRNA stability, translation and consequently higher level of protein expression in prokaryotes (Knight et al., 2001).

Western blot analyses confirmed that the PKM2 protein in tumor cells could recognize by monoclonal antibody against the M-tPKM2 (Fig. 5d), thus supporting their potential for use in the detection kits, targeted therapy or follow up of cancers.

5. Conclusions

In summary, in order to investigate the effect of antigen properties on the antibody's ability, two recombinant truncated PKM2 were designed via in silico analysis and developed to produce antibodies which can detect native PKM2. The results suggested that for the purpose of designing an antigen with the ability to produce a potent antibody against the target protein, it is better to select sequences which have a similar structure in the recombinant and native proteins, even at the cost of having shorter sequences and fewer epitopes. However, the limitation of this study was to evaluate the ability of two fragments of the target protein to produce antibodies capable of identifying a target protein. To further confirm the results of this study, more than two fragments of target protein, some of which have the same structures as the native protein whereas others have more epitopes and different structures, should be evaluated. It also would be desirable to consider different proteins for this purpose. Hence, due to the lack of similar studies in this regard, further research is required to evaluate the effect of the antigen design on the induced antibodies more accurately.

Conflicts of interest

The authors declare that they have no conflict of interest.

Acknowledgements

We would like to thank Tarbiat Modares University and Tehran University of Medical Sciences.

References

Aa, M., 2017. Epitope-based peptide vaccine design against mokola rabies virus glycoprotein g utilizing in silico. Immunome Res. 13. https://doi.org/10.4172/17457580.1000144.

Amorim, J.H., Diniz, M.O., Cariri, F.A.M.O., Rodrigues, J.F., Bizerra, R.S.P., Gonçalves, A.J.S., De Barcelos, Alves,A.M., De Souza, Ferreira,L.C., 2012. Protective immunity to DENV2 after immunization with a recombinant NS1 protein using a genetically detoxified heat-labile toxin as an adjuvant. Vaccine 30, 837–845. https://doi.org/10.1016/j.vaccine.2011.12.034.

Bameri, Z., Asadi Karam, M.R., Habibi, M., Ehsani, P., Bouzari, S., 2018. Determination immunogenic property of truncated MrpH.FliC as a vaccine candidate against urinary tract infections caused by Proteus mirabilis. Microb. Pathog. 114, 99–106. https://doi.org/10.1016/j.micpath.2017.11.015.

Bielecka, M.K., Devos, N., Gilbert, M., Hung, M.C., Weynants, V., Heckels, J.E., Christodoulides, M., 2015. Recombinant protein truncation strategy for inducing bactericidal antibodies to the macrophage infectivity potentiator protein of Neisseria meningitidis and circumventing potential cross-reactivity with human FK506-binding proteins. Infect. Immun. 83, 730–742. https://doi.org/10.1128/IAI.01815-14.

Bradford, M.M., 1976. A rapid and sensitive method for the quantitation of microgram quantities of protein utilizing the principle of protein-dye binding. Anal. Biochem. 72, 248–254. https://doi.org/10.1016/0003-2697(76)90527-3.

Chen, Z., Lu, X., Wang, Z., Jin, G., Wang, Q., Chen, D., Chen, T., Li, J., Fan, J., Cong, W., Gao, Q., He, X., 2015. Co-expression of PKM2 and TRIM35 predicts survival and recurrence in hepatocellular carcinoma. Oncotarget 6. https://doi.org/10.18632/oncotarget.2991.

Cui, R., Shi, X.-Y., 2015. Expression of pyruvate kinase M2 in human colorectal cancer and its prognostic value. Int. J. Clin. Exp. Pathol. 8, 11393–11399.

Dayton, T.L., Jacks, T., Vander Heiden, M.G., 2016. PKM2, cancer metabolism, and the road ahead. EMBO Rep. https://doi.org/10.15252/embr.201643300.

Fischer, K., dos Reis, V.P., Finke, S., Sauerhering, L., Stroh, E., Karger, A., Maisner, A., Groschup, M.H., Diederich, S., Balkema-Buschmann, A., 2016. Expression, characterisation and antigenicity of a truncated Hendra virus attachment protein expressed in the protozoan host Leishmania tarentolae. J. Virol. Methods 228, 48–54. https://doi.org/10.1016/j.jviromet.2015.11.006.

Fonseca, J.A., Cabrera-Mora, M., Singh, B., Oliveira-Ferreira, J., Da Costa, Lima-Junior, J., Calvo-Calle, J.M., Lozano, J.M., Moreno, A., 2016. A chimeric protein-based malaria vaccine candidate induces robust T cell responses against Plasmodium vivax MSP1 19. Sci. Rep. 6, 1–18. https://doi.org/10.1038/srep34527.

Gustafsson, C., Minshull, J., Govindarajan, S., Ness, J., Villalobos, A., Welch, M., 2012. Engineering genes for predictable protein expression. Protein Expr. Purif. 83, 37–46. https://doi.org/10.1016/j.pep.2012.02.013.

Knight, R.D., Freeland, S.J., Landweber, L.F., 2001. A simple model based on mutation and selection explains trends in codon and amino-acid usage and GC composition within and across genomes. Genome Biol. 4 Research0010.

Leach, A.R., 2001. Molecular Modelling: Principles and Applications, 2nd ed. Pearson Education, London.

Mohanty, N.N., Chacko, N., Biswas, S.K., Chand, K., Pandey, A.B., Mondal, B., Hemadri, D., Shivachandra, S.B., 2016. Production of recombinant non-structural protein-3 hydrophobic domain deletion (NS3ΔHD) protein of bluetongue virus from prokaryotic expression system as an efficient diagnostic reagent. Biologicals 44, 352–359. https://doi.org/10.1016/j.biologicals.2016.07.001.

Newman, Z.R., Young, J.M., Ingolia, N.T., Barton, G.M., 2016. Differences in codon bias and GC content contribute to the balanced expression of TLR7 and TLR9. Proc. Natl. Acad. Sci. 113, E1362–E1371. https://doi.org/10.1073/pnas.1518976113.

Sachdeva, S., Ahmad, G., Malhotra, P., Chauhan, V.S., Mukherjee, P., 2004. Comparison of immunogenicities of recombinant Plasmodium vivax merozoite surface protein 1 19-and 42-kiloDalton fragments expressed in Escherichia coli. Infect. … 72, 5775–5782. https://doi.org/10.1128/IAI.72.10.5775.

Shabani, S.H., Zakeri, S., Salmanian, A.H., Amani, J., Mehrizi, A.A., Snounou, G., Nosten, F., Andolina, C., Mourtazavi, Y., Djadid, N.D., 2017. Biological, immunological and functional properties of two novel multi-variant chimeric recombinant proteins of CSP antigens for vaccine development against Plasmodium vivax infection. Mol. Immunol. 90, 158–171. https://doi.org/10.1016/j.molimm.2017.06.033.

Wiederstein, M., Sippl, M.J., 2007. ProSA-web: interactive web service for the recognition of errors in three-dimensional structures of proteins. Nucleic Acids Res. 35, 407–410. https://doi.org/10.1093/nar/gkm290.

Xi, Y., Whittaker, K., 2017. Prokaryotic expression of hepatitis C Virus-NS3 protein and preparation of a monoclonal antibody. Monoclon. Antib. Immunodiagn. Immunother. 36, 251–258. https://doi.org/10.1089/mab.2017.0033.

Yang, J., Yan, R., Roy, A., Xu, D., Poisson, J., Zhang, Y., 2014. The I-TASSER suite: protein structure and function prediction. Nat. Methods 12, 7–8. https://doi.org/10.1038/nmeth.3213.

Yang, Y., Wang, F.X., Sun, N., Cao, L., Zhang, S.Q., Zhu, H.W., Guo, L., Cheng, S.P., Wen, Y.J., 2015. Development and evaluation of two truncated recombinant NP antigen-based indirect ELISAs for detection of bovine parainfluenza virus type 3 antibodies in cattle. J. Virol. Methods 222, 47–54. https://doi.org/10.1016/j.jviromet.2015.05.015.